Infection, Genetics and Evolution 74 (2019) 103933

Contents lists available at ScienceDirect

Infection, Genetics and Evolution

journal homepage: www.elsevier.com/locate/meegid

Research paper

Reciprocal control of *Mycobacterium avium* and *Mycobacterium tuberculosis* infections by the alleles of the classic Class II *H2-Aβ* gene in mice

Irina Linge, Ekaterina Petrova[1], Alexander Dyatlov, Tatiana Kondratieva, Nadezhda Logunova, Konstantin Majorov, Elena Kondratieva, Alexander Apt*

Laboratory for Immunogenetics, Central Institute for Tuberculosis, Moscow, Russia

ARTICLE INFO

Keywords:
Pathogenic mycobacteria
H2 complex
Class II genes
Lung pathology
Immune response

ABSTRACT

Genetic control of host susceptibility to *M. avium*, an important lung pathogen of immune-compromised individuals, remains incompletely defined. Apart from the *slc11a1* (*Nramp1*) gene, which plays a pivotal role in genetic control of a few intracellular pathogens, including *M. avium*, in mice, we know nothing about genetic loci determining susceptibility to and/or severity of *M. avium*-triggered disease. Previously, our lab developed a panel of *H2*-congenic, recombinant mouse strains for identification of the MHC genes involved in the control of *M. tuberculosis* infection. In the present study, we applied a few recombinant strains from this panel to study $ possible influence of allelic variations in classical Class II genes on the development of *M. avium* infection. Our results demonstrate a clear difference in lung pathology, post-infection survival time, lung neutrophil influx and corresponding chemokine/cytokine responses, as well as the degree of lung T lymphocyte activation, between mouse strains differing by the alleles of a single highly polymorphic Class II *H2-Aβ* gene. Paradoxically, mice carrying the *H2-Aβb* allele, which provides a notable protective effect against *M. tuberculosis* compared to the *H2-Aβj* allele, were more susceptible to *M. avium* infection as indicated by several parameters of the disease. We discuss possible reasons for such a reciprocal expression of phenotypes determined by a single allelic variant during two "similar" infections that may concern differences in virulence, NO-sensitivity, intracellular life style and antigenic composition between these two mycobacterial species.

1. Introduction

Mycobacterium avium is an opportunistic pathogen for humans, animals and birds, and the most common cause of non-tuberculous mycobacterial lung infection worldwide (Griffith, 2010; Griffith et al., 2007; Ignatov et al., 2012). In humans, *M. avium* pulmonary infection affects immune-compromised individuals either locally (emphysema and chronic bronchitis), or systemically (pneumonia in HIV-positive patients) (Appelberg, 2006).

Genetic control of host susceptibility to *M. avium* infection is incompletely defined. In mice, the major genetic factor of infection control is the *slc11a1* (also known as *Nramp1*) gene encoding the transmembrane protein in phagosomes which pumps out 2^+ cations, including Fe^{++}, an important nutrient of mycobacteria (Forbes and Gros, 2003; Gomes et al., 1999a, 1999b; Vidal et al., 1996). A homozygous, non-conservative G169D substitution in the AA sequence of the Slc11a1 protein completely abrogates its function and results in a high level of susceptibility to *M. avium*, as demonstrated by comparing *Nramp1*-congenic mice (Nakamura, 1992; Orme et al., 1986; Vidal et al., 1993) and by segregation genetic analysis (Kondratieva et al., 2007). The influence of the *Nramp1* gene on susceptibility to *M. tuberculosis* infection is much weaker (Nikonenko et al., 1996). In humans, los -of -function mutations in the coding sequence of the homologous *SLC11A1* gene are not known, but polymorphisms in this gene associated with susceptibility to mycobacteria are well established in different populations (discussed in (Apt et al., 2017)). However, no data are available concerning the involvement of other genes in the control of susceptibility to and/or severity of *M. avium*-triggered disease. An obvious reason for this gap in our knowledge is the relatively low virulence of the bacterium, generally considered as relatively benign for the majority of healthy, HIV-negative individuals, which explains the shortage of human resources and funding in the field.

On the other hand, numerous epidemiological, clinical and experimental studies of *M. tuberculosis* infection provide ample evidence for the polygenic nature of tuberculosis (TB) genetic and immunologic control (reviewed in Apt et al., 2017; Möller et al., 2018). Regarding

* Corresponding author at: Laboratory for Immunogenetics, Central Institute for Tuberculosis, Moscow 107564, Russia.
E-mail address: alexapt0151@gmail.com (A. Apt).
[1] Present address: Institute of Experimental Immunology, University of Zurich, Winterthurerstrasse 190, Zurich, Switzerland.

https://doi.org/10.1016/j.meegid.2019.103933
Received 18 April 2019; Received in revised form 17 June 2019
Available online 20 June 2019

experimental approaches, whole-genome association studies, performed by three independent research groups in three different combinations of parental mouse strains, demonstrated that a few quantitative trait loci (QTL) are involved in TB control (see (Apt et al., 2017) for review). Expectedly, diversity of parental strains and phenotypes chosen for the analyses resulted in different genome locations of QTLs revealed by each team, with a single notable exclusion. In two independent studies (Sánchez et al., 2003; Yan et al., 2006) a QTL involved in TB control has been mapped to the chromosomal region occupied by the *H2* complex (mouse *MHC*). Later, we showed that in our strain combination (B6 a more resistant, I/St a more susceptible partner) the *H2*-located QTL that controls TB severity is the classical Class II *H2-Aβ* gene (Logunova et al., 2015). Identification of this gene as a conspicuous factor of TB control became possible after the establishment of a panel of recombinant *H2*-congenic mouse strains bearing different small segments from the TB-susceptible I/St ($H2^j$) ancestors on the resistant B6 ($H2^b$) genetic background. Two strains from this panel possess very subtle allelic differences in the *H2* Class II region: B6·I-100 ($H2\text{-}A^jE^j$) and B6·I-139 ($H2\text{-}A^{jb}E^j$) share the identical $H2\text{-}E^j$ allele but differ by the alleles encoding the β-chain of the H2-A molecule. Remarkably, these two strains differ profoundly in susceptibility to *M. tuberculosis*, being TB-susceptible and resistant respectively (Logunova et al., 2015).

Since the involvement of the *MHC* genes in the control of *M. avium* infection has not been studied, it seemed logical to use this unique pair of congenic strains to address this issue. Importantly, our panel of strains was established on the B6 ($Nramp1^s$) genetic background. Since the $Nramp1^r$ allele is a major repressor of intracellular *M. avium* survival, minor to moderate effects of other genes, as expected in this model, would be notable only if the influence of the major genetic factor is excluded.

In the present study, we demonstrate that the Class II *H2-Aβ* gene is involved in the control of *M. avium*-triggered disease, and its allelic variations influence, albeit moderately, several features of pathology and immunity that underline the differences in infection severity. Unexpectedly, despite the not very distant genetic kinship between *M. avium* and *M. tuberculosis* (Mignard and Flandrois, 2008), *H2-Aβ* allelic phenotypes expressed during the two infections provided a mirror-like picture: a certain degree of protection against *M. tuberculosis* determined by the $H2\text{-}A\beta^b$ allelic variant as opposed to increased susceptibility to *M. avium* infection.

2. Materials and methods

2.1. Animals

Mice of the inbred recombinant *H2*-congenic strains B6·I-100 (hereafter, B100), B6·I-139 (hereafter, B139) and B6·I-9.3.19.8 developed in our lab (Logunova et al., 2015) were bred by brother-sister matings and maintained under conventional, non-SPF conditions at the Animal Facilities of the Central Institute for Tuberculosis (CIT, Moscow, Russia) in accordance with the guidelines from the Russian Ministry of Health # 755. Mouse strains were established in 2013 using a classical backcross-intercross-inbreeding scheme and PCR genotyping as described earlier (Logunova et al., 2015). To minimize genetic drift, every three generations progenies of pairs distant from the main lineage were cut off the family tree. Water and food were provided ad libitum. Female mice of 2.5 mo of age at the beginning of experiments were used. All experimental procedures were approved by the CIT Institutional Animal Care Committee.

2.2. Infection

Mice were infected with the *M. avium* strain 724R characterized earlier (Pedrosa et al., 1994), a kind gift of Dr. T. Ulrichs, Max Planck Institute for Infection Biology, Berlin. Following 3 weeks of growth in Dubos broth at 37 °C, mycobacteria were suspended in sterile saline containing 0.05% Tween 20 and kept at -80 °C until used. Mice were infected aerogenically, with $1.5–2.0 \times 10^3$ viable CFU using an Inhalation Exposure System (Glas-Col, Terre Haute, IN). Animals were exposed for 40 min to an aerosol produced by nebulizing 8 ml of a bacterial suspension in PBS solution with 0,05% Tween-80 at a concentration of 1×10^7 viable bacilli/ml. Individual body weights and mortality were monitored twice a week.

M. tuberculosis strain H37Rv, substrain Pasteur was used for axenic cultures.

2.3. CFU counts

At the indicated time points following infection, the lungs and spleens from individual mice were homogenized in 2.0 ml of sterile saline, and 10-fold serial dilutions of 0.05 ml samples were plated on Dubos agar (Difco) and incubated at 37 °C for 20–22 days before *M. avium* CFU were counted.

2.4. Histology

At the indicated time points post infection, lung tissue was examined for pathology. Mice were euthanized by a thiopental overdose. Lung tissue (left) was frozen using a –20 °C to –60 °C temperature gradient in the electronic Cryotome® (ThermoShandon, UK), and serial 6-8 μm-thick sections were made across the widest area of the lobe. Sections were stained with hematoxylin and eosin and examined by an experienced pathologist (EK) without knowledge of the experimental group. Development of fibrosis was assessed by immunohistochemistry using staining with anti-mouse SMA-Cy3 (clone 1A4, Sigma) fluorescent antibodies, followed by covering with Prolong-Gold anti-fade Immumount with DAPI (Invitrogen).

Immunohistochemical assessment of neutrophil influx was performed on lung cryosections fixed with ice-cold acetone and blocked with 10% normal mouse serum using peroxidase-conjugated anti-Ly-6G mAbs (BD-PharMingen, San Diego, CA), with hematoxylin counterstaining. All slides were examined by an experienced mouse pathologist and photographed using the Axioskop 40 microscope, AxioCam MRc5 camera and AxioVision 4.8.1.0 software for morphometry (Carl Zeiss, Berlin, Germany).

2.5. Cell suspensions

Lungs were enzymatically digested as described previously (Apt et al., 1993; Eruslanov et al., 2004). Briefly, the blood vessels were washed out by heart perfusion via cut vena cava with 0.02 mM EDTA-PBS, the lungs removed, sliced into 1–2 mm3 pieces and incubated at 37 °C for 90 min in supplemented RPMI-1640 containing 200 U/ml collagenase and 50 U/ml DNase-I (Sigma-Aldrich, MO). Single cell suspensions from 4 to 5 mice were obtained individually and washed twice in HBSS containing 2% FCS and antibiotics. 3×10^5 cells were used for assessment of surface phenotypes and the remaining sample was used for cell culture.

2.6. Cytokine ELISA

1×10^6/ml lung cells were cultured in wells of 24-well plates for 48 h in the presence of 10 μg/ml mycobacterial ultrasonic disintegrate established as previously described (Eruslanov et al., 2004). Cytokine contents in supernatants were assessed using ELISA MAX kits (Biolegend, Germany) for IL-6, IL-10, IFN-γ and TGF-α, and DuoSetELISA kits (R&D systems, USA) for TGF-β according to the manufacturers' instructions.

Immune cell phenotypes were evaluated by flow cytometry using the following labeled antibodies in different combinations:

From Biolegend, San Diego, CA: PerCp-anti-CD4 (clone GK 1.5),

APC-anti-CD8 (clone 53–6.7), FITC-anti-CD44 (clone IM7), PE-anti-CD62L (clone MEL-14), FITC-antiLy-6G (clone 1A8), PE-anti-F4/80 (clone BM8), AF488-CD19 (clone 6D5).

For intracellular IFN-γ staining, 1.5×10^6 cells were cultured in 24-well plates in the presence of 10 μg/ml mycobacterial sonicate for 48 h; GolgiPlug block (1 μl/ml; BD Biosciences) was added for the last 10 h. Cells were then stained with anti-IFN-γ mAb XMG1.2 (BD Biosciences) using the Cytofix/Cytoperm kit (BD Biosciences).

2.7. T cell proliferative response

Lymphocytes were obtained from the popliteal lymph nodes of 100 and 139 mice immunized by injection into the rear footpads of 10 μg/mouse of *M. avium* sonicate mixed 1:1 with incomplete Freund's adjuvant. At day 21 following immunization, lymph node cells were purified by negative selection using magnetic beads ($CD4^+$ T-cell Isolation kit II, Miltenyi Biotec) according to the manufacturer's recommendations. To assess antigen-specific proliferation, 10^5 purified $CD4^+$ T cells were co-cultured with 2×10^5 mitomycin C-treated splenic antigen-presenting cells (APC) in a 96-well flat-bottom plate (Costar), at 37 °C, 5% CO2, in supplemented RPMI-1640 containing 10 μg/ml of *M. avium* sonicate. Non-stimulated wells served as controls. Triplicate cultures were pulsed with 0.5 μCi [^{3}H]-thymidine for the last 18 h of 40 h incubation. The label uptake was measured in a liquid scintillation counter (Wallac, Finland) after harvesting the well's contents onto fiberglass filters using a semi-automatic cell harvester (Scatron, Norway).

Macrophage cultures, IFN-γ stimulation, and evaluation of NO production were performed exactly as described earlier for the *M. tuberculosis* system (Majorov et al., 2003), except that multiplicities of infection (MOI) of macrophage cultures were higher (10–100:1) because of the much lower virulence of *M. avium* compared to *M. tuberculosis*. To block NO production, cultures were supplemented with 100 mM of specific inhibitor L-NIL (L-N^6-(1-Iminoethyl) lysine, Sigma-Aldrich, MO). Chemical NO donor DETA/NO (Diethylenetriamine, Sigma-Aldrich, MO) at concentrations indicated in Fig. 7 was used in axenic mycobacterial cultures.

3. Results

3.1. Mice of the B139 strain developed more severe disease after M. avium infection

First, in mice of the B100 and B139 strains, we assessed the most prominent features of chronic mycobacterial infections: dynamics of cachexia, life span post infection, CFU counts in organs and lung pathology. After respiratory *M. avium* challenge, B139 mice developed cachexia more rapidly and died earlier compared to B100 mice (Fig. 1A, B). However, there were no inter-strain differences in lung CFU counts (Fig. 1C), and splenic CFU counts differed significantly, albeit slightly, only on week 8 post challenge (Fig. 1D).

Despite the lack of differences in *M. avium* multiplication in lungs of B100 and B139 mice, estimation of lung pathology and fibrosis during infection provided information supporting survival data. At week 8 post infection, diffuse inflammation of the lung tissue was observed in 139 mice (Fig. 2A, bottom), whereas in B100 mice infectious foci were well delineated from relatively normal tissue (Fig. 2A, top). At the late stage of infection (18 weeks), B139 mice displayed significantly larger necrotic lesions compared to B100 mice (Fig. 2B, D). These lesions were surrounded by fibrotic tissue, and, expectedly, fibrotic zones were larger in B139 mice (Fig. 2C). Thus, mice of the two strains clearly differed by manifestations of lung pathology at the early and late phases of the infectious course. Taken together, our results demonstrate that mice of the B100 strain carrying *j* alleles of the Class II genes were more resistant to *M. avium* infection compare to B139 mice, which is in a sharp contrast to *M. tuberculosis* infection, which provided a reciprocal picture (Logunova et al., 2015).

3.2. Inflammation and cytokine production in the lungs

Positive roles of early inflammation and granuloma formation in host defense are well established for *M. tuberculosis* infection in the mouse, guinea pig, and macaque models (Kondratieva et al., 2018; Lin et al., 2006; Turner et al., 2003). To assess what factors are involved in the earlier lung granuloma formation in B100 mice after *M. avium* infection, we estimated the level of key pro- and anti-inflammatory

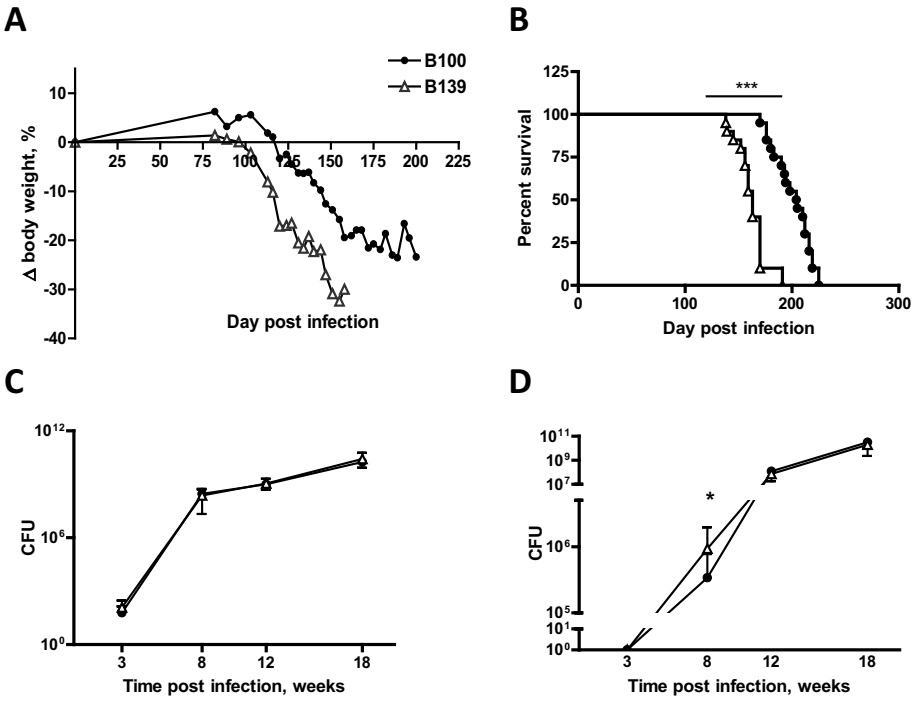

Fig. 1. Major parameters of *M. avium* infection in B100 and B139 mice. Cachexia (A), mortality (B) and bacillary loads (C, D) following infection. (A, B) – One of 3 similar independent experiments (N = 12–15 mice per group each, ***P < .0001, Log-rank test); CFU counts in lungs (C) and spleens (D) were assessed for 4–5 mice per group per time point in 3–4 independent experiments which provided similar results. (D) – *P < .05 (Student's t-test).

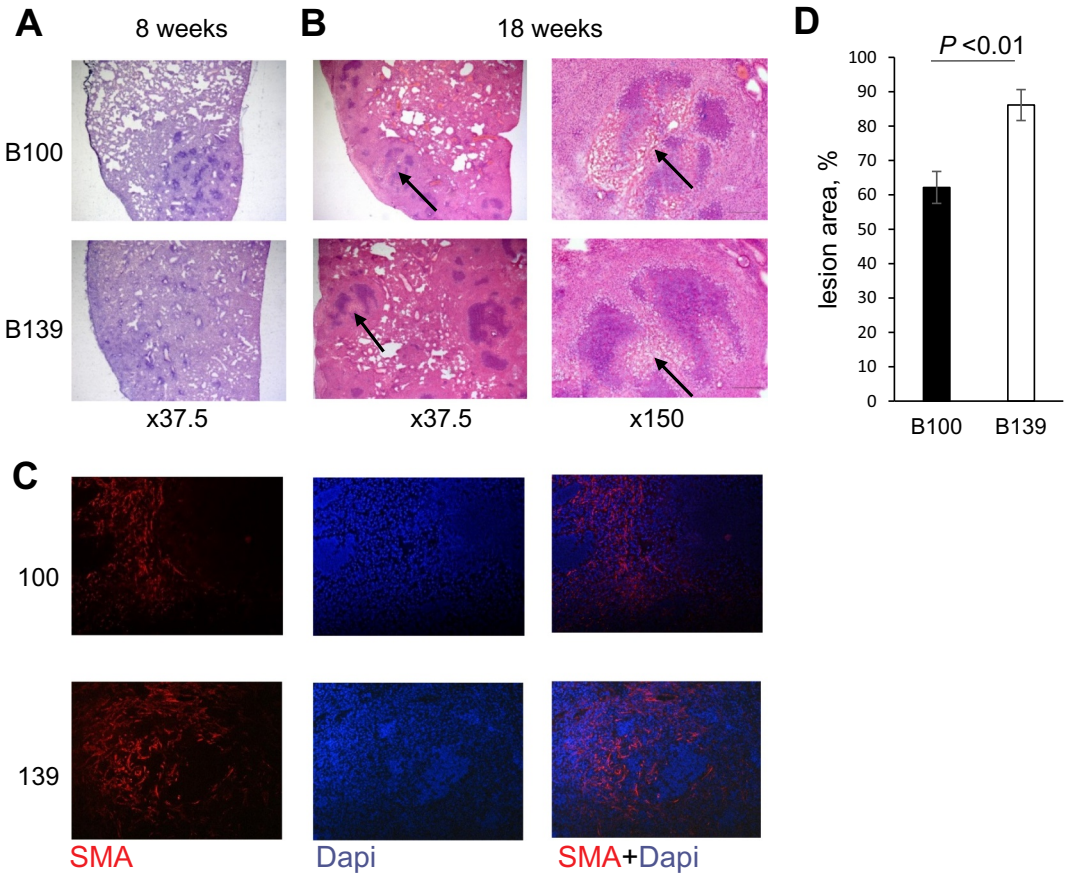

Fig. 2. Lung histopathology at indicated time points post challenge. (A) – delineated inflammatory foci in B100 (top) and diffuse inflammation in B139 (bottom) mice at week 8 post infection. Necrotic inflammation (arrows) was more massive in B139 mice at week 18 post infection (B), and occupied larger areas of the lung according to morphometry (D) performed with the morphometric tool for the Zeiss Axioscop40 microscope (6–7 slices per lung, 4–5 mice per group, results of one representative experiment of three total are presented). (C) – Visualization of fibrotic areas with anti-SMA-Cy3 antibodies (red). Lung cryosections were obtained at week 18 post challenge and fixed with 4% PFA. Slides were mounted using ProLong Gold anti-fade reagent with DAPI for nuclei staining (blue), magnification ×600. (For interpretation of the references to colour in this figure legend, the reader is referred to the web version of this article.)

cytokines produced by the lung cells. As shown in Fig. 3A, lung cells of B100 mice secreted more pro-inflammatory TNF-α in response to *M. avium* antigens, compared to their B139 counterparts. However, there were no significant inter-strain differences in the production of pro-inflammatory IL-6 (Fig. 3B) and IFN-γ (Fig. 3C), or anti-inflammatory IL-10 (Fig. 3D) at the early stage of infection. TGF-β was below the detection limit in both strains (data not shown). No significant inter-strain differences in cytokine production were detected at 18 weeks of infection (data not shown). Again, the whole picture of the early response differed from that observed for *M. tuberculosis* infection, after which significantly higher levels of all major type 1 pro-inflammatory cytokines, TNF-α, IL-6, and IFN-γ, were produced by lung cells of more resistant mice, strain 139 in this case (Logunova et al., 2015).

3.3. Lung neutrophil influx

In several experimental settings, it was demonstrated that during *M. tuberculosis* infection, neutrophils infiltrating infected lung tissue play a deleterious rather than a protective role (Dallenga et al., 2017; Eruslanov et al., 2005; Yeremeev et al., 2015). Since the role of neutrophils in *M. avium*-triggered disease is incompletely defined, we assessed the level of neutrophil inflammation in the lungs of infected B100 and B139 animals. Surprisingly, we observed a higher level of neutrophil influx in the lungs of more resistant mice at week 8 post-infection, as assessed by flow cytometry and immune staining (Fig. 4A, B). Interestingly, no differences in total numbers of $CD4^+$ and $CD8^+$ T cells, B cells and macrophages between mice of the two strains were found (data not shown). We then tried to find a mechanistic explanation for the higher level of neutrophil migration to the lungs of B100 mice. To this end, we compared lung tissue samples from infected 100 and 139 mice for the expression of genes encoding a few molecules playing major roles in neutrophil mobilization to mycobacteria-infected lungs – IL-17, CXCL-1, and CXCL-2 (Lombard et al., 2016). As shown in Fig. 4C, the level of expression of all three genes was higher in 100 mice at week 8 of infection. At later stages of infection, lung neutrophil influx gradually increased and did not differ between mice of the two strains (data not shown).

3.4. H2-A allelic variants and T-cell responses: In vitro and in vivo phenotypes

Since our model system is based upon mouse strains that differ only by the allelic variants of the H2-A molecule presenting mycobacterial antigens to $CD4^+$ T-cells, it was logical to address the question about possible dependence of the disease phenotypes described above on variations in T cell responses during infection. We first directly compared capacities of the *M. avium*-specific $CD4^+$ T cells from mice of the two strains to recognize and respond to a mixture of *M. avium* antigens in vitro. Both B100 and B139 $CD4^+$ T cells readily proliferated in response to *M. avium* antigens presented by syngenic APC. Moreover, notable, albeit diminished, antigen-specific proliferation of highly purified B100 and B139 cells was induced in the presence of allogenic APC (Fig. 5A). This was never observed in response to *M. tuberculosis* antigens, where all specific $CD4^+$ T cells appeared to be *H2-A*-restricted

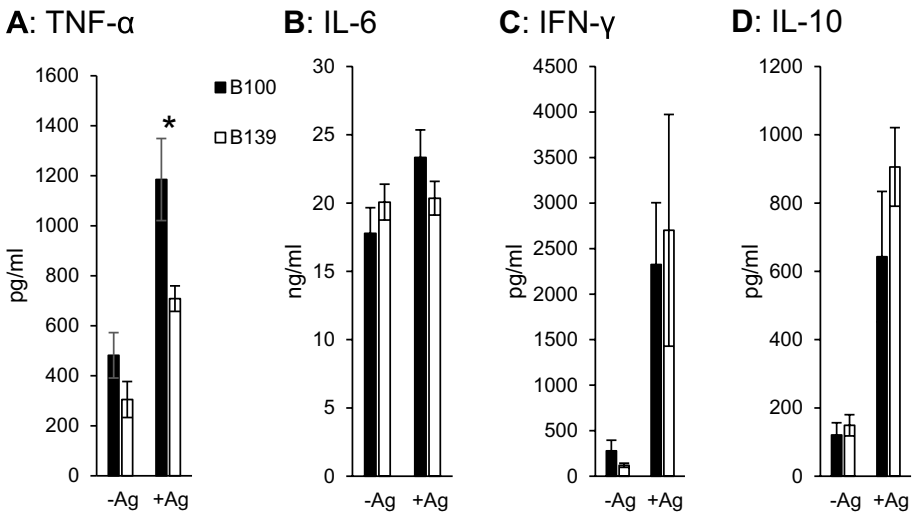

Fig. 3. Cytokine production by lung cells. Suspensions of lung cells obtained from B100 and B139 mice at week 8 post challenge were cultured for 48 h in the presence (AG+) or absence (AG-) of *M. avium* antigens. Cytokine contents (A – TNF-α; B – IL-6; C – IFN-γ; D – IL-10) in supernatants were assessed in the ELISA format for 4–5 individual mice per each group. The results of one of two similar experiments are displayed as mean ± SEM. *$P < .05$ (Student's *t*-test).

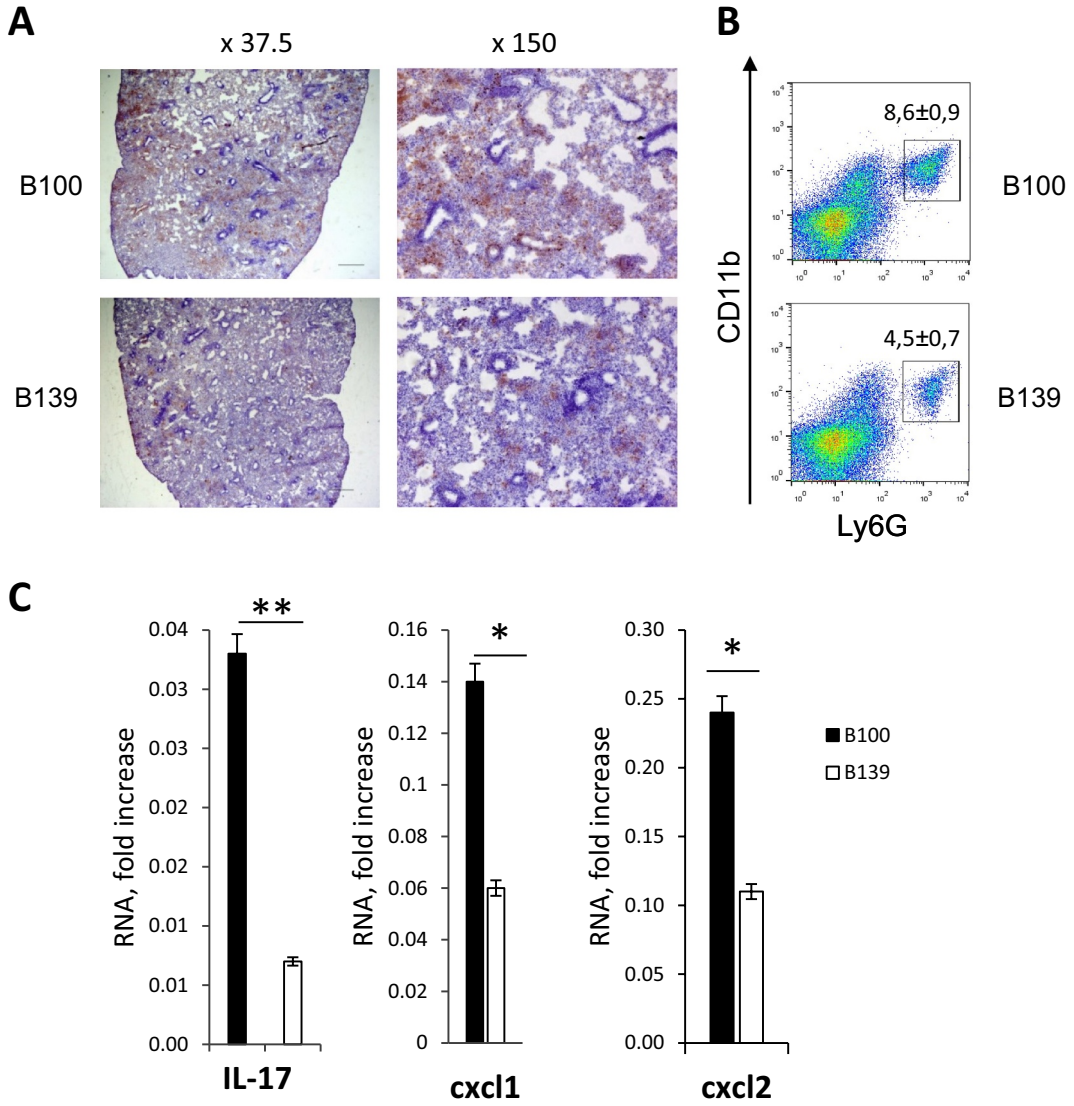

Fig. 4. Increased neutrophil inflammation in lungs of B100 mice at week 8 of infection. (A) – staining of lung cryosections with anti-Ly-6G mAbs, magnifications ×37 (left) and ×150 (right), brown peroxidase staining. (B) – FACS analysis of lung cells, neutrophils gated as $Ly6G^+CD11b^+$ population, percent of neutrophils to the whole lung cell population is provided for 100 and 139 mice ($P < 0,04$ - statistics). (C) – Higher expression of genes encoding major neutrophil attractants in 100 mice: IL-17 (left), CXCL1 (middle) and CXCL2 (right). Quantitative real-time PCR assay normalized to the *hprt* and *actinb* housekeeping genes. 4–5 individual mice per group, 1 of 2–3 similar independent experiments. (For interpretation of the references to colour in this figure legend, the reader is referred to the web version of this article.)

(Logunova et al., 2015). We hypothesized that, in contrast to *M. tuberculosis*, *M. avium* antigens may be presented in the context of the H2-E molecule, whose *j* allele is identical in B100 and B139 mice, thus explaining cross-presentation. Indeed, when we used APC from another congenic mouse strain from the same panel, B6·I-9.3.198, bearing the *H2-A*^{j}*H2-E*^{null} allelic composition, T cells obtained from B100 (*H2-A*^{j}) mice continued to respond to antigenic stimulation, whereas recognition by the B139 (*H2-A*^{jb}) cells was abrogated (Fig. 5A). Thus, we revealed yet another difference in the genetic control of the two infections: T cell recognition of *M. tuberculosis* antigens develops in the context of a single Class II molecule (H2-A), but *M. avium* antigens are presented by both H2-A and H2-E molecules.

We then compared the dynamics of the lung T cell populations during the infection. The absolute numbers of CD4^{+} and CD8^{+} T cells in the lungs remained stable and did not differ between B100 and B139 mice throughout infection (Fig. 5B). However, two important parameters of T cell immunity clearly demonstrated inter-strain differences. First, both CD4^{+} and CD8^{+} T cell populations in more resistant B100 mice contained significantly more activated (CD44^{hi}CD62L^{lo}), i. e. recently recruited and continuing to respond, cells compare to more susceptible B139 mice (Fig. 5C). Second, the numbers of antigen-specific, IFN-γ-producing CD4^{+} T cells in the lungs and spleens was higher in B100 compared to B139 mice at week 18 post-challenge (Fig. 5D). Moreover, analogous experiments performed in the parental, *H2-E*-negative *H2-A*^{b} B6 strain and its recombinant *H2-E*-negative, *H2-A*^{j} B6·I-9.3.19.8 derivative strain clearly demonstrated that the *H2-A*-determined antigen-specific IFN-γ production is responsible for the inter-strain differences, and that the *H2-A*^{j} allelic variant is associated with higher numbers of IFN-γ-producing CD4+ T cells in both organs (Fig. 5E). Taken together, these observations suggest that more resistant mice retain adaptive, protective, H2-A^{j}-dependent T cell immune response in infected organs for a longer time.

3.5. Macrophages of B100 and B139 mice: M. avium Growth, IFN-γ stimulation, NO production

Macrophages are generally considered to be key cells providing a number of microbicidal actions which contain mycobacterial growth

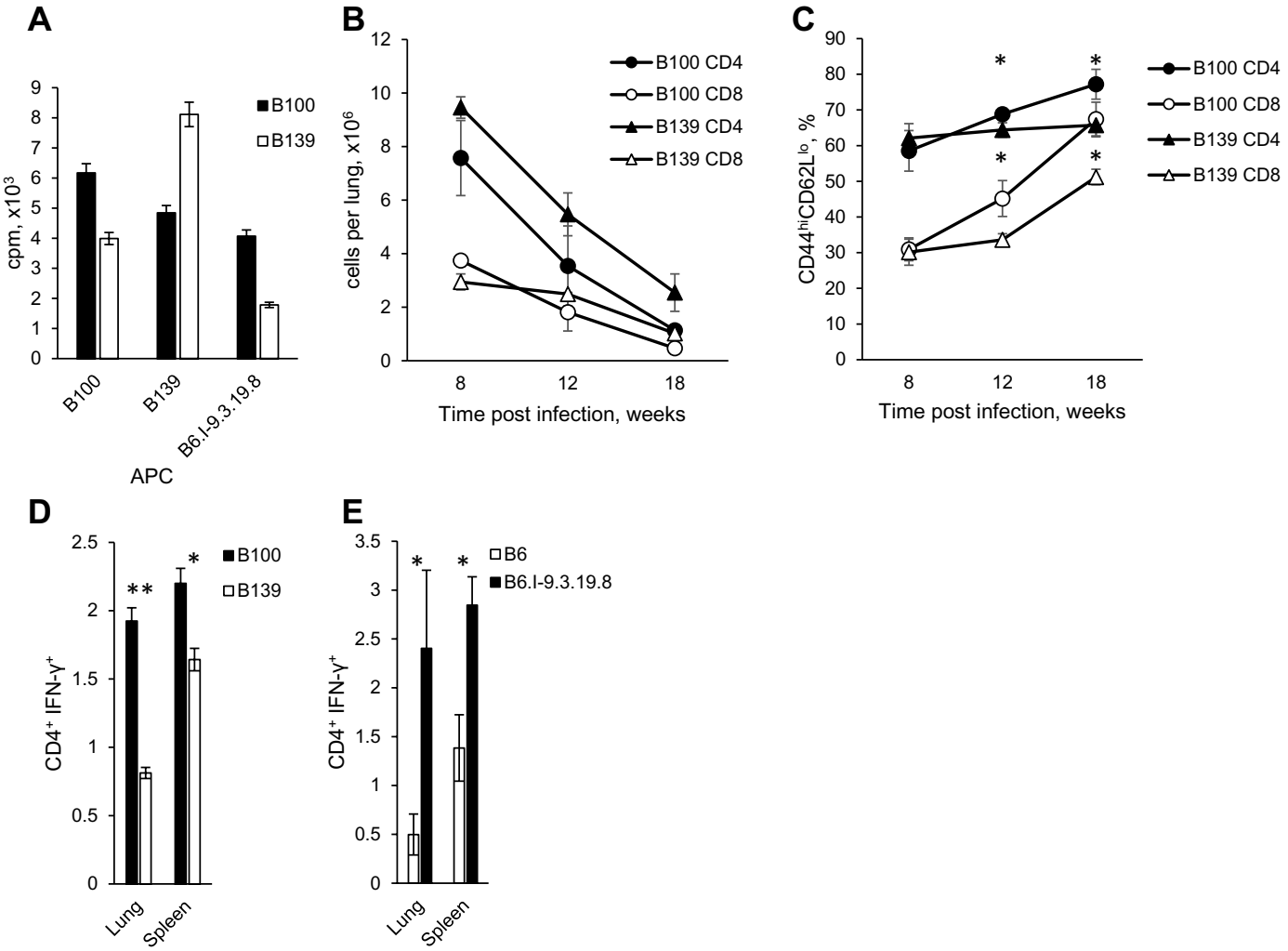

Fig. 5. Characterization of T cells from B100 and B139 mice. (A) – CD4^{+} T cells recognize *M. avium* antigens in the context of both H2-A and H2-E molecules. APC from mice bearing different allelic Class II combinations were able to induce antigen-specific proliferation in vitro of highly purified immune lymph node CD4^{+} T cells (B100 – black bars, B139- white bars) in the H2-A- and H2-*E*-restricted manner (see text for details). Results from one of two similar independent experiments are expressed as mean ± SEM of triplicate cultures. (ΔCPM = mean CPM_{Ag+} − mean CPM_{Ag-} cultures). (B) The numbers of CD4+ and CD8+ lung T cells did not differ between B100 and B139 mice throughout infection. (C) – Larger amounts of activated (CD44^{hi}CD62L^{lo}) CD4^{+} and CD8^{+} were present in the lungs of B100 mice at weeks 12 and 18 of infection (*$P < .05$, Student's *t*-test, per cent of the total CD4^{+} and CD8^{+} populations, as assessed by FACS). (D, E) – The *H2-A*^{j} allelic variant was associated with higher numbers of IFN-γ-producing CD4+ T cells in the lungs and spleens and this phenotype was independent of the expression of the H2-E molecule (D – B100 and B139 mice are H2-E-positive, E – B6 and 9.3.19.8 mice are H2-E-negative). Results of one of two similar experiments (total $N = 9$) are shown as mean cell number per organ ± SEM, with statistics for 4–5 individual mice per group. *$P < .05$, **$P < .01$, Student's *t*-test.

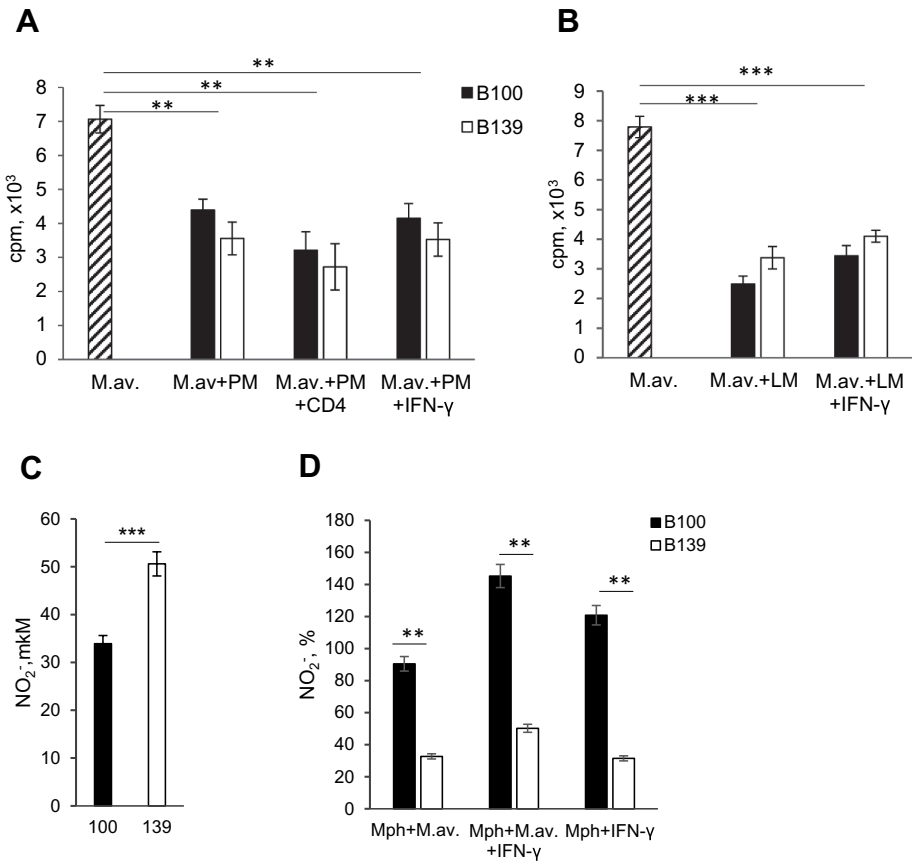

Fig. 6. Antibacterial activity of macrophages from B100 and B139 mice. Cultured macrophages obtained from peritoneal cavities (A – 5 days after peptone injection, PM) or infected lung tissue (B – week 14 post *M. avium* infection, LM) of B100 and B139 mice displayed neither inter-strain differences in spontaneous bacteriostatic capacity, nor increased activity after addition of immune CD4$^+$ T cells or IFN-γ. Results are shown as mean CPM ± SEM of [^{3}H]-uracil incorporation for the MOI = 50 (MOI titration – 100, 50, 25, 12.5, 6.25) in 72-h cultures, *M. avium* alone - striped bar. Spontaneous NO production in lung macrophages from infected B100 mice was lower than in B139 macrophages (C) but dramatically increased in response to external IFN-γ and/or *M. avium* cells (D). See Materials and Methods for details. Two summarized independent experiments with 4–5 mice per group each. Student's *t*-test, $P < .05$*, < 0.01**, < 0.001***.

(O'Garra et al., 2013). The lack of differences between the lung *M. avium* CFU counts in B100 and B139 mice (Fig. 1) suggested that the bactericidal functions of macrophages from mice of the two strains were similar. However, since the genetic difference between the strains concerns the Class II *H2-Aβ* gene involved in T cell activation (Fig. 5), we decided to compare B100 and B139 macrophage bacteriostatic functions in two different types of *M. avium*-infected cell cultures: pure macrophages vs. macrophages plus immune CD4$^+$ T cells. As shown in Fig. 6A, peptone-attracted peritoneal macrophages from the mice of both strains displayed similar moderate bacteriostatic effects which depended neither on the presence of immune CD4$^+$ T cells nor on the presence of external IFN-γ.

Anticipating that bacteriostatic activity of artificially activated peritoneal macrophages may not reflect the processes developing in activated lung macrophages during real infection, we then checked the activity of lung macrophages obtained from mice at chronic stages of the disease. As shown in Fig. 6B, lung macrophages recovered from 18wk-infected B100 and 139 mice did not differ in anti-*M. avium* activity irrespective of the presence of immune T cells and external IFN-γ.

It is well known that IFN-γ-activated macrophages elevate inducible nitric oxide synthase (iNOS) expression with subsequent release of nitric oxide (NO) known to be one of the main natural agents against *M. tuberculosis* in mice (Macmicking et al., 1997). On the other hand, it was clearly demonstrated that *M. avium* is resistant to NO action (Gomes et al., 1999a, 1999b; Tomioka et al., 1997). Since a higher level of IFN-γ secretion by CD4$^+$ T cells from B100 mice was detected (Fig. 5), we assessed the level of NO production by lung macrophages from infected animals at the chronic stage of infection. Lung macrophages extracted from B100 mice spontaneously produced less NO compared to B139 macrophages (Fig. 6C). However, additional in vitro stimulation of macrophages with live *M. avium* and/or IFN-γ increased profoundly NO production by B100, but not B139 macrophages (Fig. 6D).

To find out whether the level of NO production directly influences *M. avium* survival, we performed a series of experiments in an attempt to either block NO production or provide an extracellular source of reactive nitrogen. As shown in Fig. 7A, blockage of NO-production in IFN-γ-stimulated lung macrophages with specific low m. w. inhibitor NIL did not alter their moderate bacteriostatic capacities.

One possible explanation of *M. avium* resistance to NO within macrophages could be physical separation between bacilli and the NO source: unlike *M. tuberculosis*, *M. avium* cannot escape from phagosomes due to a deletion of the RD1 genomic region (van Ingen et al., 2009), whereas the location of iNOS is cytosolic. To check this possibility, we supplemented axenic *M. avium* and *M. tuberculosis* cultures with the chemical NO donor DETA/NO and estimated survival of bacteria by measuring [^{3}H]-uracil uptake. As shown in Fig. 7B, a moderate decrease in *M. avium* viability was observed at DETA/NO concentrations 25–50-fold higher than those sufficient for a sub-total inhibition of [^{3}H]-uracil uptake by *M. tuberculosis* cells. This result provides direct evidence that, unlike *M. tuberculosis*, *M. avium* is resistant to reactive nitrogen intermediates.

Taken together, our results demonstrate that allelic differences in the H2-A molecule influence, albeit moderately, progression of the *M. avium*-triggered disease, and that T cell-dependent variations in the degree of lung tissue inflammation, rather than the control of bacterial populations, account for the differences in major “late” phenotypes – survival time and lung tissue necrosis.

4. Discussion

Despite mycobacterial diseases having a long history of being studied, their genetic control by the host is still poorly characterized. This is especially true for infection induced by *M. avium* – a less virulent and less thoroughly investigated mycobacterial agent. In fact, the *Nramp1* gene is the only well-established regulator of *M. avium* infection (Kondratieva et al., 2007; Nakamura, 1992; Orme et al., 1986; Vidal

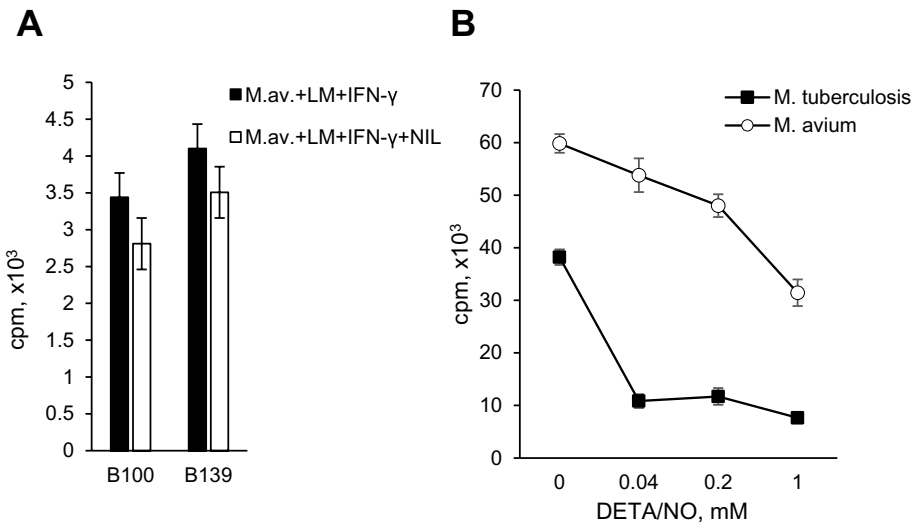

Fig. 7. *M. avium* is resistant to the bactericidal activity of NO. (A) – Survival of *M. avium* within lung macrophages (LM) from mice of the two strains, as measured by the [^{3}H]-uracil incorporation, did not change after IFN-γ stimulation (black bars) or NO blocking with specific L-NIL inhibitor (white bars). Results are shown for MOI = 50. (B) –Direct inhibitory effect of NO provided by the DETA/NO donor onto *M. avium* was weak and required very high DETA/NO concentrations compared to *M. tuberculosis*. Results obtained in axenic mycobacterial cultures are shown for the initial bacterial load 5×10^5 CFU per well.

et al., 1993). However, *M. avium* is an important pathogen for immune compromised individuals (Appelberg, 2006), and gaining new knowledge about genetic control of the corresponding infection may shed more light on its pathogenesis and host immunity. Here we demonstrate that the classical Class II *H2-Aβ* gene, whose involvement in TB control was identified previously (Logunova et al., 2015), is also involved in the control of *M. avium* infection. Paradoxically, allelic variants of this gene influence progression of two infections in opposite directions: mice carrying the *H2-Aβ*^{b} allele (strain B139) are more resistant to TB compared to mice of the B100 (*H2-Aβ*^{j}) strain, whereas the latter are more resistant to *M. avium*, as indicated by the expression of two major disease phenotypes – life span and lung pathology (Figs. 1, 2).

Additional evidence for prominently different consequences of host interactions with the two mycobacterial species was obtained by comparing the protective vs. deleterious role of neutrophil migration toward locations of invading pathogens in the lung. A negative role of neutrophil inflammation during TB infection was convincingly demonstrated in several studies (Mishra et al., 2017; Nandi and Behar, 2011; Yeremeev et al., 2015), and recently neutrophilic areas of inflammation were described as predominant sites of *M. tuberculosis* replication in mice (Mishra et al., 2017). On the other hand, the protective role of neutrophils in response against *M. avium* was demonstrated in in vivo neutrophil depletion experiments performed in *M. avium*-susceptible C57BL/6 mice (Appelberg et al., 1995). In the present work, we show that a massive, early lung neutrophil influx, accompanied by a higher expression of genes encoding neutrophil attractants CXCL1, CXCL2, and IL-17, characterizes mice of the B100 strain which are more resistant to *M. avium* (Fig. 4). Different roles of neutrophils in the two mycobacterial infections may be due to a difference in virulence of the two species. It is well established that murine and human neutrophils effectively engulf but poorly kill intracellular *M. tuberculosis* (Berry et al., 2010; Corleis et al., 2012; Eruslanov et al., 2005). However, bactericidal capacities of neutrophils might be sufficient for diminishing the growth of much less virulent *M. avium*, which lacks the RD1 locus containing genes for the major mycobacterial virulence and immune dominant factors (Ganguly et al., 2008).

The two mouse strains under study differ exclusively by the allelic variants of the Class II H2-Aβ molecule operating via the presentation of antigenic peptides recognized by the CD4$^+$ T lymphocytes to drive proliferation and IFN-γ production. Although the dogma of a protective role of CD4$^+$ T cell-derived IFN-γ in tuberculous lung tissue was recently challenged (Sakai et al., 2016), a detailed analysis of slowly developing TB infection caused by a genetically attenuated *M. tuberculosis* strain in mice confirmed the protective nature of this pathway (Kondratieva et al., 2018). In addition, it was convincingly shown that protection against *M. tuberculosis* provided by CD4$^+$ T cell-secreted IFN-γ is based not only on macrophage activation but also on impaired neutrophil survival in the lungs due to the inhibition of IL-17 production (Nandi and Behar, 2011). Results for *M. avium* infection presented herein illustrate remarkable differences in the genetic regulation and pathogenesis of the two infections along with the CD4$^+$ T cell – IFN-γ – neutrophil axis. Indeed, carriers of the "*M. tuberculosis*-susceptible" *H2-Aβ*^{j} allele appeared to be *M. avium*-resistant (Figs. 1, 2) and displayed massive lung neutrophil influx and higher *il17a* gene expression (Fig. 4), despite increased amounts of activated, IFN-γ-producing lung T cells (Fig. 5). This is in sharp contrast to data obtained previously for *M. tuberculosis* infection (Logunova et al., 2015; Nandi and Behar, 2011).

One of the reasons why the two infections induce such a divergent picture of host response and pathology, which is easy to suggest but difficult to prove directly, is a diverse antigenic composition of the two mycobacterial species. *M. tuberculosis* and *M. avium* are distant enough phylogenetically to accumulate differences in their proteomes and lipidomes sufficient for a significant discrepancy in antigenic structure. The lack of the Exs-5 secretion system (RD1 locus) in the *M. avium* genome mentioned above is a good example. Indirect evidence of the existence of such antigenic differences is provided by our results on the *H2* restriction of antigen recognition in the two models of infection. When we checked the capacity of CD4$^+$ T cells to recognize *M. avium* antigens in the context of different allelic variants of the MHC Class II molecules, it appeared that these antigens are effectively presented not only by the H2-A but also by the H2-E molecules (Fig. 5). This is completely different from the presentation of *M. tuberculosis* antigens, which occurs exclusively in the context of the H2-A molecule (Logunova et al., 2015). However, physical elution from Class II molecules loaded with *M. tuberculosis* and *M. avium* antigen cocktails and characterization of peptide profiles will be needed to directly prove this hypothesis – a task that is extremely expensive and laborious.

Yet another difference between the two mycobacterial infections concerns the efficacy of T cell-macrophage interactions in mycobacterial killing and the role of NO production in this process. Neither activated, *M. avium*-specific CD4$^+$ T cells, nor external IFN-γ elevated the capacity of macrophages to constrain *M. avium* growth (Fig. 6), which again differs from analogous activities in the *M. tuberculosis* system (Logunova et al., 2015). This discrepancy may be due to serious differences between the two mycobacterial species regarding sensitivity to NO production by the host cells. The key action of IFN-γ on infected macrophages is activation of iNOS with subsequent elevation of NO production. Reactive nitrogen intermediates are known as essential *M. tuberculosis*-killing compounds for decades in mice (Nathan and Xie, 1994). On the other hand, in many studies exploring different strains of

M. avium, it was shown that these bacteria are resistant to NO (Flórido et al., 1999; Lousada et al., 2006; Pearl et al., 2012; Tomioka et al., 1997). Moreover, iNOS−/− mice appeared to be even more resistant to highly virulent *M. avium* compared to the wild type mice (Gomes et al., 1999a, 1999b). We also did not find any sign of NO anti-*M. avium* activity in our experiments exploring NO-blocking and NO-supplying strategies (Fig. 7).

Overall, our data suggest that the host response to the two mycobacterial pathogens is differentially regulated by the alleles of the Class II *H2-Aβ* gene. However, the sequence of immune and inflammatory reactions follows a somewhat stereotypic pattern in a "blind" manner. The evolutionary fixed set of interrelated innate and acquired immune reactions against mycobacterial pathogens provides a moderate degree of allele-specific protection against *M. tuberculosis* but is not effective against *M. avium* despite the lower virulence of this species. Our conclusions concern fine genetic differences with moderate to weak influences on infectious immunity. However, at the populational level, such subtle variations resulting from recombination events within certain immunologically active genetic regions may be more important for gradual evolutionary shifts than nonsense or missense mutations that produce phenotypes that are extreme and subjected to rapid elimination by natural selection.

Declaration of Competing Interest

The authors have no competing interests to declare.

Acknowledgments

This work was financially supported by the Russian Federal Program 0515-2019-0018 and by the Russian Science Foundation (RSF) grant 18-45-04015 (to AA, biological markers of inflammation and lung pathology). We are grateful to Prof. David McMurray for critically reading the manuscript.

References

Appelberg, R., 2006. Pathogenesis of Mycobacterium avium infection: typical responses to an atypical Mycobacterium? Immunol. Res. 35, 179–190. https://doi.org/10.1385/IR:35:3:179.

Appelberg, R., Castro, A.G., Gomes, S., Pedrosa, J., Silva, M.T., 1995. Susceptibility of beige mice to Mycobacterium avium: role of neutrophils. Infect. Immun. 63, 3381–3387.

Apt, A.S., Avdienko, V.G., Nikonenko, B.V., Kramnik, I.B., Moroz, A.M., Skamene, E., 1993. Distinct H-2 complex control of mortality, and immune responses to tuberculosis infection in virgin and BCG-vaccinated mice. Clin. Exp. Immunol. 94, 322–329.

Apt, A.S., Logunova, N.N., Kondratieva, T.K., 2017. Host genetics in susceptibility to and severity of mycobacterial diseases. Tuberculosis 106, 1–8. https://doi.org/10.1016/j.tube.2017.05.004.

Berry, M.P.R., Graham, C.M., McNab, F.W., Xu, Z., Bloch, S.A.A., Oni, T., Wilkinson, K.A., Banchereau, R., Skinner, J., Wilkinson, R.J., Quinn, C., Blankenship, D., Dhawan, R., Cush, J.J., Mejias, A., Ramilo, O., Kon, O.M., Pascual, V., Banchereau, J., Chaussabel, D., O'Garra, A., 2010. An interferon-inducible neutrophil-driven blood transcriptional signature in human tuberculosis. Nature 466, 973–977. https://doi.org/10.1038/nature09247.

Corleis, B., Korbel, D., Wilson, R., Bylund, J., Chee, R., Schaible, U.E., 2012. Escape of Mycobacterium tuberculosis from oxidative killing by neutrophils. Cell. Microbiol. 14, 1109–1121. https://doi.org/10.1111/j.1462-5822.2012.01783.x.

Dallenga, T., Repnik, U., Corleis, B., Eich, J., Reimer, R., Griffiths, G.W., Schaible, U.E., 2017. M. tuberculosis-induced necrosis of infected neutrophils promotes bacterial growth following phagocytosis by macrophages. Cell Host Microbe 22, 519–530. e3. https://doi.org/10.1016/j.chom.2017.09.003.

Eruslanov, E.B., Majorov, K.B., Orlova, M.O., Mischenko, V.V., Kondratieva, T.K., 2004. Lung cell responses to *M. tuberculosis* in genetically susceptible and resistant mice following intratracheal challenge. Clin. Exp. Immunol. 135, 19–28. https://doi.org/10.1046/j.1365-2249.2004.02328.x.

Eruslanov, E.B., Lyadova, I.V., Tatiana, K., Majorov, K.B., Scheglov, I.V., Orlova, M.O., Apt, A.S., Kondratieva, T.K., 2005. Neutrophil responses to mycobacterium tuberculosis infection in genetically susceptible and resistant mice neutrophil responses to *Mycobacterium tuberculosis* infection in genetically susceptible and resistant mice. Infect. Immun. 73, 1744–1753. https://doi.org/10.1128/IAI.73.3.1744.

Flórido, M., Gonçalves, A.S., Silva, R.A., Ehlers, S., Cooper, A.M., Appelberg, R., 1999. Resistance of virulent *Mycobacterium avium* to gamma interferon-mediated antimicrobial activity suggests additional signals for induction of mycobacteriostasis. Infect. Immun. 67, 3610–3618.

Forbes, J.R., Gros, P., 2003. Iron, manganese, and cobalt transport by Nramp1 (Slc11a1) and Nramp2 (Slc11a2) expressed at the plasma membrane. Blood 102, 1884–1892. https://doi.org/10.1182/blood-2003-02-0425.

Ganguly, N., Siddiqui, I., Sharma, P., 2008. Role of *M. tuberculosis* RD-1 region encoded secretory proteins in protective response and virulence. Tuberculosis 88, 510–517. https://doi.org/10.1016/j.tube.2008.05.002.

Gomes, M.S., Dom, G., Pedrosa, J., Boelaert, J.R., Appelberg, R., 1999a. Effects of iron deprivation on *Mycobacterium avium* growth. Tuber. Lung Dis. 79, 321–328. https://doi.org/10.1054/tuld.1999.0216.

Gomes, M.S., Flórido, M., Pais, T.F., Appelberg, R., 1999b. Improved clearance of *Mycobacterium avium* upon disruption of the inducible nitric oxide synthase gene. J. Immunol. 162, 6734–6739.

Griffith, D.E., 2010. Nontuberculous mycobacterial lung disease. Curr. Opin. Infect. Dis. 23, 185–190. https://doi.org/10.1097/QCO.0b013e328336ead6.

Griffith, D.E., Aksamit, T., Brown-Elliott, B.A., Catanzaro, A., Daley, C., Gordin, F., Holland, S.M., Horsburgh, R., Huitt, G., Iademarco, M.F., Iseman, M., Olivier, K., Ruoss, S., von Reyn, C.F., Wallace, R.J., Winthrop, K., 2007. An official ATS/IDSA statement: diagnosis, treatment, and prevention of nontuberculous mycobacterial diseases. Am. J. Respir. Crit. Care Med. 175, 367–416. https://doi.org/10.1164/rccm.200604-571ST.

Ignatov, D., Kondratieva, E., Azhikina, T., Apt, A., 2012. *Mycobacterium avium*-triggered diseases: pathogenomics. Cell. Microbiol. 14, 808–818. https://doi.org/10.1111/j.1462-5822.2012.01776.x.

Kondratieva, E.V., Evstifeev, V.V., Kondratieva, T.K., Petrovskaya, S.N., Pichugin, A.V., Rubakova, E.I., Averbakh, M.M., Apt, A.S., 2007. I/St mice hypersusceptible to *Mycobacterium tuberculosis* are resistant to *M. avium*. Infect. Immun. 75, 4762–4768. https://doi.org/10.1128/IAI.00482-07.

Kondratieva, T., Kapina, M., Rubakova, E., Kondratieva, E., Nikonenko, B., Majorov, K., Dyatlov, A., Linge, I., Apt, A., 2018. A new model for chronic and reactivation tuberculosis: infection with genetically attenuated *Mycobacterium tuberculosis* in mice with polar susceptibility. Tuberculosis (Edinb) 113, 130–138.

Lin, P.L., Pawar, S., Myers, A., Pegu, A., Fuhrman, C., Reinhart, T.A., Capuano, S.V., Klein, E., Flynn, J.L., 2006. Early events in *Mycobacterium tuberculosis* infection in cynomolgus macaques. Infect. Immun. 74, 3790–3803. https://doi.org/10.1128/IAI.00064-06.

Logunova, N., Korotetskaya, M., Polshakov, V., Apt, A., 2015. The QTL within the *H2* Complex involved in the control of tuberculosis infection in mice is the classical Class II *H2-Ab1* Gene. PLoS Genet. 11, e1005672. https://doi.org/10.1371/journal. pgen.1005672.

Lombard, R., Doz, E., Carreras, F., Epardaud, M., Le Vern, Y., Buzoni-Gatel, D., Winter, N., 2016. IL-17RA in non-hematopoietic cells controls CXCL-1 and 5 critical to recruit neutrophils to the lung of mycobacteria-infected mice during the adaptive immune response. PLoS One. https://doi.org/10.1371/journal.pone.0149455.

Lousada, S., Flórido, M., Appelberg, R., 2006. Regulation of granuloma fibrosis by nitric oxide during *Mycobacterium avium* experimental infection. Int. J. Exp. Pathol. 87, 307–315. https://doi.org/10.1111/j.1365-2613.2006.00487.x.

Macmicking, J.D., North, R.J., Lacourse, R., Mudgett, J.S., Shah, S.K., Nathan, C.F., 1997. Identification of nitric oxide synthase as a protective locus against tuberculosis. Proc. Natl. Acad. Sci. U. S. A. 94, 5243–5248.

Majorov, K.B., Lyadova, I.V., Kondratieva, T.K., Eruslanov, E.B., Rubakova, E.I., Orlova, M.O., Mischenko, V.V., Apt, A.S., 2003. Different innate ability of I/St and A/Sn mice to combat virulent Mycobacterium tuberculosis: phenotypes expressed in lung and extrapulmonary macrophages. Infect. Immun. 71, 697–707.

Mignard, S., Flandrois, J.P., 2008. A seven-gene, multilocus, genus-wide approach to the phylogeny of mycobacteria using supertrees. Int. J. Syst. Evol. Microbiol. 58, 1432–1441. https://doi.org/10.1099/ijs.0.65658-0.

Mishra, B.B., Lovewell, R.R., Olive, A.J., Zhang, G., Wang, W., Eugenin, E., Smith, C.M., Yao, J.P., Long, J.E., Dubuke, M.L., Palace, S.G., Goguen, J.D., Baker, R.E., Nambi, S., Mishra, R., Booty, M.G., Baer, C.E., Shaffer, S.A., Dartois, V., Mccormick, B., Chen, X., Sassetti, C.M., 2017. Nitric oxide prevents a pathogen permissive granulocytic inflammation during tuberculosis HHS Public Access. Nat. Microbiol. https://doi.org/10.1038/nmicrobiol.2017.72.

Möller, M., Kinnear, C.J., Orlova, M., Kroon, E.E., van Helden, P.D., Schurr, E., Hoal, E.G., 2018. Genetic resistance to *Mycobacterium tuberculosis* infection and disease. Front. Immunol. 9, 2219. https://doi.org/10.3389/fimmu.2018.02219.

Nakamura, R.M., 1992. Effect of natural resistance gene on the immune response against *Mycobacterium avium* complex infection. Kekkaku 67, 41–46.

Nandi, B., Behar, S.M., 2011. Regulation of neutrophils by interferon-γ limits lung inflammation during tuberculosis infection. J. Exp. Med. 208, 2251–2262. https://doi.org/10.1084/jem.20110919.

Nathan, C., Xie, Q.W., 1994. Nitric oxide synthases: roles, tolls, and controls. Cell 78, 915–918.

Nikonenko, B.V., Apt, A.S., Mezhlumova, M.B., Avdienko, V.G., Yeremeev, V.V., Moroz, A.M., 1996. Influence of the mouse *Bcg*, *Tbc-1* and *xid* genes on resistance and immune responses to tuberculosis infection and efficacy of bacille Calmette-Guérin (BCG) vaccination. Clin. Exp. Immunol. 104, 37–43.

O'Garra, A., Redford, P.S., McNab, F.W., Bloom, C.I., Wilkinson, R.J., Berry, M.P.R., 2013. The immune response in tuberculosis. Annu. Rev. Immunol. 31, 475–527. https://doi.org/10.1146/annurev-immunol-032712-095939.

Orme, I.M., Stokes, R.W., Collins, F.M., 1986. Genetic control of natural resistance to nontuberculous mycobacterial infections in mice. Infect. Immun. 54, 56–62.

Pearl, J.E., Torrado, E., Tighe, M., Fountain, J.J., Solache, A., Strutt, T., Swain, S., Appelberg, R., Cooper, A.M., 2012. Nitric oxide inhibits the accumulation of CD4 + CD44hiTbet + CD69lo T cells in mycobacterial infection. Eur. J. Immunol. 42, 3267–3279. https://doi.org/10.1002/eji.201142158.

Pedrosa, J., Flórido, M., Kunze, Z.M., Castro, A.G., Portaels, F., McFadden, J., Silva, M.T., Appelberg, R., 1994. Characterization of the virulence of *Mycobacterium avium* complex (MAC) isolates in mice. Clin. Exp. Immunol. 98, 210–216.

Sakai, S., Kauffman, K.D., Sallin, M.A., Sharpe, A.H., Young, H.A., Ganusov, V.V., Barber, D.L., 2016. CD4 T cell-derived IFN-γ plays a minimal role in control of pulmonary *Mycobacterium tuberculosis* infection and must be actively repressed by PD-1 to prevent lethal disease. PLoS Pathog. 12, 1–22. https://doi.org/10.1371/journal.ppat.1005667.

Sánchez, F., Radaeva, T.V., Nikonenko, B.V., Persson, A.-S., Sengul, S., Schalling, M., Schurr, E., Apt, A.S., Lavebratt, C., 2003. Multigenic control of disease severity after virulent *Mycobacterium tuberculosis* infection in mice. Infect. Immun. 71, 126–131. https://doi.org/10.1128/IAI.71.1.126-131.2003.

Tomioka, H., Sato, K., Sano, C., Akaki, T., Shimizu, T., Kajitani, H., Saito, H., 1997. Effector molecules of the host defence mechanism against *Mycobacterium avium* complex: the evidence showing that reactive oxygen intermediates, reactive nitrogen intermediates, and free fatty acids each alone are not decisive in expression of macrophage an. Clin. Exp. Immunol. 109, 248–254. https://doi.org/10.1046/j.1365-2249.1997.4511349.x.

Turner, O.C., Basaraba, R.J., Orme, I.M., 2003. Immunopathogenesis of pulmonary granulomas in the Guinea pig after infection with *Mycobacterium tuberculosis*. Infect. Immun. 71, 864–871.

van Ingen, J., de Zwaan, R., Dekhuijzen, R., Boeree, M., van Soolingen, D., 2009. Region of difference 1 in nontuberculous Mycobacterium species adds a phylogenetic and taxonomical character. J. Bacteriol. 191, 5865–5867. https://doi.org/10.1128/JB.00683-09.

Vidal, S.M., Malo, D., Vogan, K., Skamene, E., Gros, P., 1993. Natural resistance to infection with intracellular parasites: isolation of a candidate for Bcg. Cell 73, 469–485.

Vidal, S.M., Pinner, E., Lepage, P., Gauthier, S., Gros, P., 1996. Natural resistance to intracellular infections: Nramp1 encodes a membrane phosphoglycoprotein absent in macrophages from susceptible (Nramp1 D169) mouse strains. J. Immunol. 157, 3559–3568.

Yan, B.-S., Kirby, A., Shebzukhov, Y.V., Daly, M.J., Kramnik, I., 2006. Genetic architecture of tuberculosis resistance in a mouse model of infection. Genes Immun. 7, 201–210. https://doi.org/10.1038/sj.gene.6364288.

Yeremeev, V., Linge, I., Kondratieva, T., Apt, A., 2015. Neutrophils exacerbate tuberculosis infection in genetically susceptible mice. Tuberculosis 95, 447–451. https://doi.org/10.1016/j.tube.2015.03.007.